Surface Morphology, Molecular Reorientation, and Liquid Crystal Alignment Properties of Rubbed Nanofilms of a Well-Defined Brush Polyimide with a Fully Rodlike Backbone

Boknam Chae,[†] Seung Bin Kim,*[,†] Seung Woo Lee,[‡] Sang Il Kim,[‡] Wooyoung Choi,[‡] Byeongdu Lee,[‡] Moonhor Ree,*[,‡] Kyung Hoon Lee,[§] and Jin Chul Jung*[,§]

Department of Chemistry, BK21 Functional Polymer Thin Film Group, Center for Integrated Molecular Systems, Polymer Research Institute, Department of Materials Science & Engineering, and Center for Advanced Functional Polymers, Pohang University of Science & Technology, San 31, Hyoja-dong, Pohang 790-784, Republic of Korea

Received April 24, 2002

ABSTRACT: Nanoscaled films of poly{*p*-phenylene 3,6-bis[4-(*n*-butoxy)phenyloxy]pyromellitimide} (C4-PMDA-PDA PI), a well-defined brush polyimide (PI) composed of aromatic−aliphatic bristles set into a fully rodlike polymer backbone (two bristles per chemical repeat unit of the polymer backbone), were studied by atomic force microscopy, optical retardation, prism coupling, and linearly polarized IR spectroscopy before and after mechanical rubbing with velvet fabric, and their liquid crystal (LC) aligning abilities were investigated. Uniform, homogeneous LC alignment was achieved at the rubbed film surfaces of PIs with positively birefringent characteristics. Surprisingly, however, the LC alignment director for this PI is perpendicular to the rubbing direction as well as to the reorientation direction of the polymer main chains. This is the first time that LCs on a PI surface have been induced to align in the direction perpendicular to the rubbing direction, a significant departure from the LC alignment observed for all other PI materials reported so far, for which LC alignment is always parallel to the rubbing direction. This unusual LC alignment is attributed to the strength of the anisotropic intermolecular interactions of the LC molecules with the short bristles attached perpendicularly to the polymer chain, which override the interactions with the main polymer chains and with the microgroove lines with fine grooves that are created along the rubbing direction. The LC pretilt angle is expected to be 25−55° with respect to a direction perpendicular to the rubbing direction, although this angle could not be determined due to the limitations of the crystal-rotation apparatus employed. In particular, the *n*-butyl end group of the bristle was found to play a critical role in the pretilting of LC molecules, as well as in the perpendicular LC alignment. In addition, the surface morphology of the rubbed PI films was investigated in detail, with particular consideration being given to the polymer property characteristics, the structure of the velvet fabric fibers, and the rubbing conditions.

Introduction

One of the most recently developed and important applications of polyimides (PIs) is their use in liquid crystal (LC) alignment layers for LC flat-panel display devices.[1] PIs are widely used as LC alignment layers because of their advantageous properties, such as excellent optical transparency, adhesion, heat resistance, dimensional stability, and insulation.[2,3] Such PI film surfaces need to be treated if they are to produce a uniform alignment of LC molecules with a defined range of pretilt angle values.[1] At present, a rubbing process using a rayon velvet fabric (i.e., a cellulose fabric) is the only technique adopted in the LC display industry to treat PI film surfaces for the mass-production of flat-panel LC display devices. This process has become the method of choice because of its simplicity and the controllability with this method of both the LC anchoring energy and the pretilt angle.[4,5] Much effort has been exerted to understand the mechanism behind the alignment of LC molecules on the rubbed polymer surface. A variety of factors have been proposed to explain the surface anchoring and alignment mechanism of the LC molecules: (1) microgrooves in connection with anisotropic LC orientational elasticity via steric interaction,[6,7] (2) polymer molecules from the velvet fabric deposited and oriented on the alignment layer surface during the rubbing process,[8,9] (3) surface electric fields,[10] (4) anisotropically reoriented polymer chains,[2,3,5,8,11−14] (5) a near-surface order parameter different from that of the bulk LC molecules,[12,15] and (6) coupling of a bending mode of the LC director to the surface electric fields (i.e., flexoelectricity).[16] Of these suggestions, the two models for the alignment process that have received the most attention are the microgroove mechanism[6,7] and the anisotropic polymer chain reorientation mechanism,[2,3,5,8,11−14] although the exact mechanism of LC alignment is still a subject of debate.

In addition to the uniform, unidirectional alignment of LC molecules, their pretilt angle (i.e., their out-of-plane tilt angle) plays the most important role[1] in determining the optical and electrical performance of the industrial LC display devices that currently use nematic LC molecules. Much effort has also been expended to achieve the desired LC pretilt angle and to understand the mechanism behind LC pretilt phenomena. Some investigators have proposed that the out-

* To whom all correspondence should be addressed. Telephone: +82-54-279-2106 (SBK); 279-2120 (MR). Fax: +82-54-279-3399. E-mail: sbkim@postech.edu; ree@postech.edu.

[†] Department of Chemistry and BK21 Functional Polymer Thin Film Group.

[‡] Department of Chemistry, BK21 Functional Polymer Thin Film Group, Center for Integrated Molecular Systems, and Polymer Research Institute.

[§] Polymer Research Institute, Department of Materials Science & Engineering, and Center for Advanced Functional Polymers.

10.1021/ma020639i CCC: $22.00
Published on Web 12/07/2002

of-plane LC tilt angle is governed by van der Waals interactions between the LC molecules and the alkyl side chains of the polyimide.[2,3,17] In contrast, other investigators have suggested that LC pretilt is determined by the polymer backbone structure but is independent of the length of the side chains.[18,19] The exact mechanism controlling the LC pretilt angle on rubbed surfaces has not yet been unambiguously elucidated.

There are two natural locations on the PI main chain for attaching side chains, the diamine unit and the dianhydride unit. Thus far, a number of the former case[2,3,11−14,20] but few examples of the latter case have been reported. Although pyromellitic dianhydride is the most commonly used dianhydride monomer in the synthesis of aromatic polyimides, only the additions of relatively short substituents such as phenyl, methyl, phenyloxy, halogen, and trifluoromethyl to its 3- or 6-position have been reported.[21] In previous work[22] we presented the first report of the preparation of monomeric 3,6-bis[4-(*n*-alkyloxy)phenyloxy]pyromellitic dianhydrides (C*m*-PMDAs: $m = 1, 4, 8, 12$, where m is the number of carbons in the *n*-alkyloxy group) and of their polyimides from various diamines. That work focused mainly on the synthesis and characterization of the fundamental properties of these PIs.

For the present study we chose poly{*p*-phenylene 3,6-bis[4-(*n*-butoxy)phenyloxy]pyromellitimide} (C4-PMDA-PDA PI) from the various C*m*-PMDA-based PIs synthesized in our laboratories because of its easily controlled structural features; it is a well-defined brush polymer composed of aromatic−aliphatic bristles set into a fully rodlike polymer backbone (two bristles per chemical repeat unit of the polymer backbone), which displays unique LC alignment characteristics, different from those of the conventional PI alignment layer materials reported thus far in the literature. To better understand the mechanism of LC alignment by the C4-PMDA-PDA PI surface, we measured the surface orientational distributions both of the main chains and of the bristles (i.e., side groups) of the PI film before and after rubbing, using optical phase retardation analysis and linearly polarized FTIR spectroscopy, and we also examined the film surface topography using atomic force microscopy. In addition, antiparallel LC cells were assembled with the rubbed films and injected with a nematic LC, 4-*n*-pentyl-4′-cyanobiphenyl (5CB), and the alignment behavior of the LC molecules was characterized. We discuss the observed LC alignment taking into account the interactions between the reoriented PI chains and the LC molecules. In addition, the contribution of the film surface topography to LC alignment is discussed.

Experimental Section

Materials and Film Preparation. A poly(amic acid) (PAA) precursor of C4-PMDA-PDA PI (shown in Figure 1) was prepared in *N*-methylpyrrolidone (NMP) from the respective dianhydride and PDA, according to the method described in our previous work.[22] The PAA precursor had an inherent viscosity of 0.81 at a concentration of 0.1 g/dL in NMP at 25.0 °C. The PI films were prepared by spin-casting of the PAA solution onto calcium fluoride (CaF_2) windows (25 mm diameter × 2 mm thick) for FTIR spectra, gold-coated silicon wafers (15 mm × 10 mm) for AFM images, and indium tin oxide (ITO) glasses for optical retardation and LC cell assembly, followed by drying on a hot plate at 80 °C for 1 h. The dried PAA precursor films were thermally imidized in an oven under dry nitrogen gas flow at 250 °C for 2 h. The resulting PI films were measured to have a thickness of around 200 nm, using a spectroscopic ellipsometer (J. A. Woollam Company, model M-44) and an α-stepper (Veeco Company, model Tektak3). The polyimide films coated onto substrates were rubbed with varying rubbing density (L/l)[3,7,13] using a laboratory rubbing machine (Wande Company) with a roller covered by a rayon velvet fabric (Yoshikawa Company, YA-20-R):

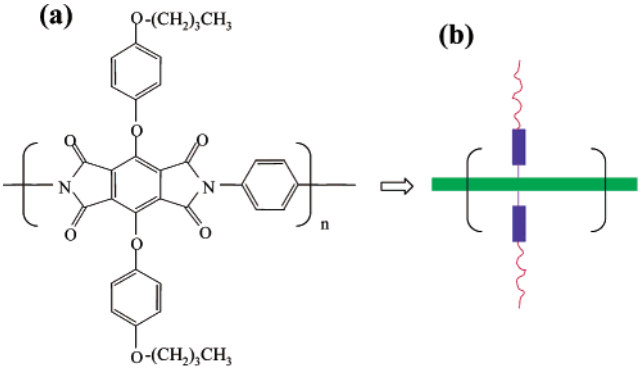

C4-PMDA-PDA PI

Figure 1. (a) Chemical structure of a fully rodlike polyimide containing 4-*n*-butoxyphenyloxy side groups (C4-PMDA-PDA PI). (b) Schematic structure of a well-defined brush C4-PMDA-PDA PI, composed of two bristles per chemical repeat unit on a rodlike polymer backbone.

$$\frac{L}{l} = N\left(\frac{2\pi rn}{60v} - 1\right) \tag{1}$$

where L is the total length of the rubbing cloth which contacts a certain point of the polymer film (mm), l is the contact length of the circumference of rubbing roller (mm), N is the cumulative number of rubbings, n and r are the speed (rpm) of and the radius (cm) of the rubbing roller (rpm), and v is the velocity (cm/s) of the substrate stage. The velvet fabric has a density of 24 000 fibers per cm^2, and each fiber has a dimension of 1.85 mm height × 15 μm diameter. In addition, relatively thick PI films (around 5 μm thick) were prepared on cover slide glasses for refractive index measurements.

LC Cells. Some of the rubbed PI films on glass substrates were cut into 2.5 cm × 2.5 cm pieces. Paired pieces from the same glass substrate were assembled together in the antiparallel rubbing direction by using 50 μm thick spacers. A nematic LC, 5CB (Aldrich Chemical Co.) containing 1.0 wt % Disperse Blue 1 (Aldrich Chemical Co.) as a dichroic dye, was injected into the cell gap, followed by sealing of the injection hole with an epoxy glue. The LC cells were then heat-treated for 5 min at 40 °C, which is slightly higher than the nematic-to-isotropic transition temperature of 5CB, to remove any flow-induced memory possibly induced by the LC injection process. The prepared LC cells were examined to be homogeneous through the whole cell by optical microscopy.

Measurements. Surface images were captured using an atomic force microscope (AFM) (ThermoMicroscopes Company, model AutoProbe CP Research) in noncontact mode. An ultralever cantilever (17 N/m spring constant and 320 kHz resonance frequency) was used for scanning, with a tip-to-sample distance of 10−40 nm. Image processing and data analysis were performed using the IP 2.0 software program provided by ThermoMicroscopes Company. Optical phase retardations were measured using an optical setup with a photoelastic modulator (PEM) (Hinds Instruments, model PEM90) with a fused silica head, a He−Ne laser of 632.8 nm wavelength (Spectra-Physics, Model 106-1), a pair of polarizers (Oriel, Model 27300), a photodiode detector (UDT Sensors, Model PIN-10DL), and a pair of lock-in amplifiers (Stanford Research Systems, model SR510), as described elsewhere.[23] Samples were installed perpendicular to the incident beam direction. While rotating the sample, optical phase retardations were measured as a function of the angle of rotation. Fourier transform infrared (FTIR) spectroscopic measurements were carried out on a Bomem DA8 FTIR spectrometer equipped

with a polarizer (single-diamond polarizer, Harrick Scientific). Samples were installed perpendicular to the incident beam direction. While the polarizer was being rotated, IR spectra were recorded at 4 cm^{-1} resolution with a liquid-nitrogen-cooled mercury cadmium telluride (MCT) detector under vacuum, as a function of the angle of rotation, and interferograms were accumulated 256 times. The LC alignment in the cell was examined by measuring the absorption of the linearly polarized He−Ne laser beam (632.8 nm wavelength) as a function of the rotational angle of the cell, allowing the construction of polar diagrams. For this measurement the LC cell was installed perpendicular to the incident laser beam direction. The pretilt angle α of the LC molecules was measured using a crystal rotation apparatus made in our laboratory, which was controlled by a personal computer and equipped with a goniometer, a photodiode detector, a He−Ne laser (632.8 nm), a polarizer and analyzer pair, and a sample stage.[3,13] In addition, refractive index measurements were performed for the PI films of around 5.0 μm thickness using a prism coupler equipped with a He−Ne laser source of 632.8 nm wavelength (i.e., 474.08 THz) controlled by a personal computer.[24] The refractive index in the film plane (n_{xy}) was measured in the transverse electric mode, whereas the refractive index out-of-plane (n_z) was obtained in the transverse magnetic mode. All measurements were performed using a cubic zirconia prism of $n = 2.1677$ at a wavelength of 632.8 nm.

Results and Discussion

Surface Morphology. Using the AFM technique, we examined in detail the surfaces of C4-PMDA-PDA PI films before and after they had been rubbed with a rubbing density of 180. Figure 2 shows the surface morphology of a C4-PMDA-PDA PI film before rubbing treatment. The film surface is apparently covered with submicrometer-scaled spikes (see Figure 2a). When the film is examined at the nanoscale, the surface shows an orange-peel-like morphology with a periodicity of around 600 nm (see Figure 2b). The root-mean-square (rms) roughness is 0.5 nm over the area of 5×5 μm^2. The surface morphology and roughness of the PI film derive mainly from the characteristics of the polymer chains that govern the aggregation and molecular ordering that occur during the drying and thermal imidization processes after spin-casting. Of course, the surface morphology might also partly reflect the surface roughness of the gold-coated substrates we employed.

Figure 3 presents AFM images of the surface of a rubbed C4-PMDA-PDA PI film. As seen in Figure 3a, microgroove lines, which are produced by the rubbing process, are aligned parallel to the rubbing direction. The typical microgroove line has a width of around 2.2 μm, which corresponds to the width of the surface area contacted during the rubbing process by a fiber filament with a diameter of 15 μm. This observation supports the conclusion that the microgroove lines were generated through shear-induced deformation of the polymer film surface induced by the contact of fibers during the rubbing process, as observed for other rubbed polymer films.[5] Each microgroove line consists of valley lines at the two edges and a hill line with a flat area, all oriented along the rubbing direction. The height difference between the valley and the hill is approximately 20 nm. The rms surface roughness across the microgroove lines is 14.9 nm (see Figure 3b), which is much larger than that of the unrubbed film surface. Figure 3d shows a surface profile taken across the microgroove line along the thin, long line. In particular, the surface profile measured from the flat area of the hill in the microgroove oscillates with a periodicity of around 100 nm in the region 350−850 nm (along the *x*-axis). The appearance of such a periodic oscillation in the surface profile is evidence of the presence within the microgroove of microroughness at a scale of around 100 nm. Such microroughness is also discernible in Figure 3c, although that is weakly developed along the rubbing direction. The presence of microroughness is reflected in the surface of the flat area of the hill in the microgroove, which has a rms roughness of 2.8 nm, still larger than that of the unrubbed film surface. The formation of such microroughness could be due to the fiber structure of the velvet fabric. Each fiber of the velvet fabric has a diameter of 15 μm, but each fiber tip consists of subfibrous filaments that have a broad range of diameters, from a few submicrometers to a few micrometers.[25] The subfibrous filaments at the fiber end might generate microroughness in the film surface by their contact with the film surface during the rubbing process. Microroughness formation might also result in part from the deformation response of the PI film to the shear force produced by the fibers during the rubbing process.

The observed surface morphology does not fully resemble the morphologies of rubbed films prepared from the commercialized PI alignment layer materials with flexible polymer backbones.[26] Submicrogroove lines composed of microroughness are observed but are only very weakly developed in the rubbed C4-PMDA-PDA PI film, yet they are found to be well developed on the rubbed surfaces of the PIs used commercially for LC alignment.[26] This difference in surface morphology might result from differences in the deformation responses of the different PI films to the shear force caused by the contact of fibers during the rubbing process. For example, the hardness or ductility of a polymer may directly correlate to its response to the shear-induced deformation process. In general, under shear process conditions a harder polymer is less deformed, producing only weakly developed structure, while a more ductile polymer is deformed more easily, producing relatively well developed structure. Taking into account this correlation between hardness and ductility with shear deformation, the observed surface morphology for C4-PMDA-PDA PI films suggests that these films exhibit greater hardness than commercial PIs based on flexible backbone structures.

In addition to the groove structures described above, a sharp, clifflike wall is clearly discernible along the third microgroove line from the left in Figure 3a for the rubbed C4-PMDA-PDA PI film. It is unlikely that such a clifflike wall (or valley) along the microgroove line was formed only via shear-induced deformation of the PI film caused by fiber contact during rubbing. Such a clifflike wall may be evidence that some degree of abrasion accompanies the shear-induced PI deformation of the rubbing process.

Refractive Index and Optical Retardation. For an unrubbed film of the PI with 5.0 μm thickness, in-plane and out-of-plane refractive indices (n_{xy} and n_z) were measured at 632.8 nm. The PI film exhibits $n_{xy} = 1.655$ and $n_z = 1.629$. The PI film exhibits anisotropic refractive indices; that is, the out-of-plane birefringence Δ_{xy-z} ($=n_{xy} - n_z$) is 0.026. In general, because of their long chain character, polymer molecules in thin films have a tendency to lie in the film plane, resulting in an out-of-plane birefringence in the PI film.[24] This tendency of polymer in-plane orientation increases strongly as the

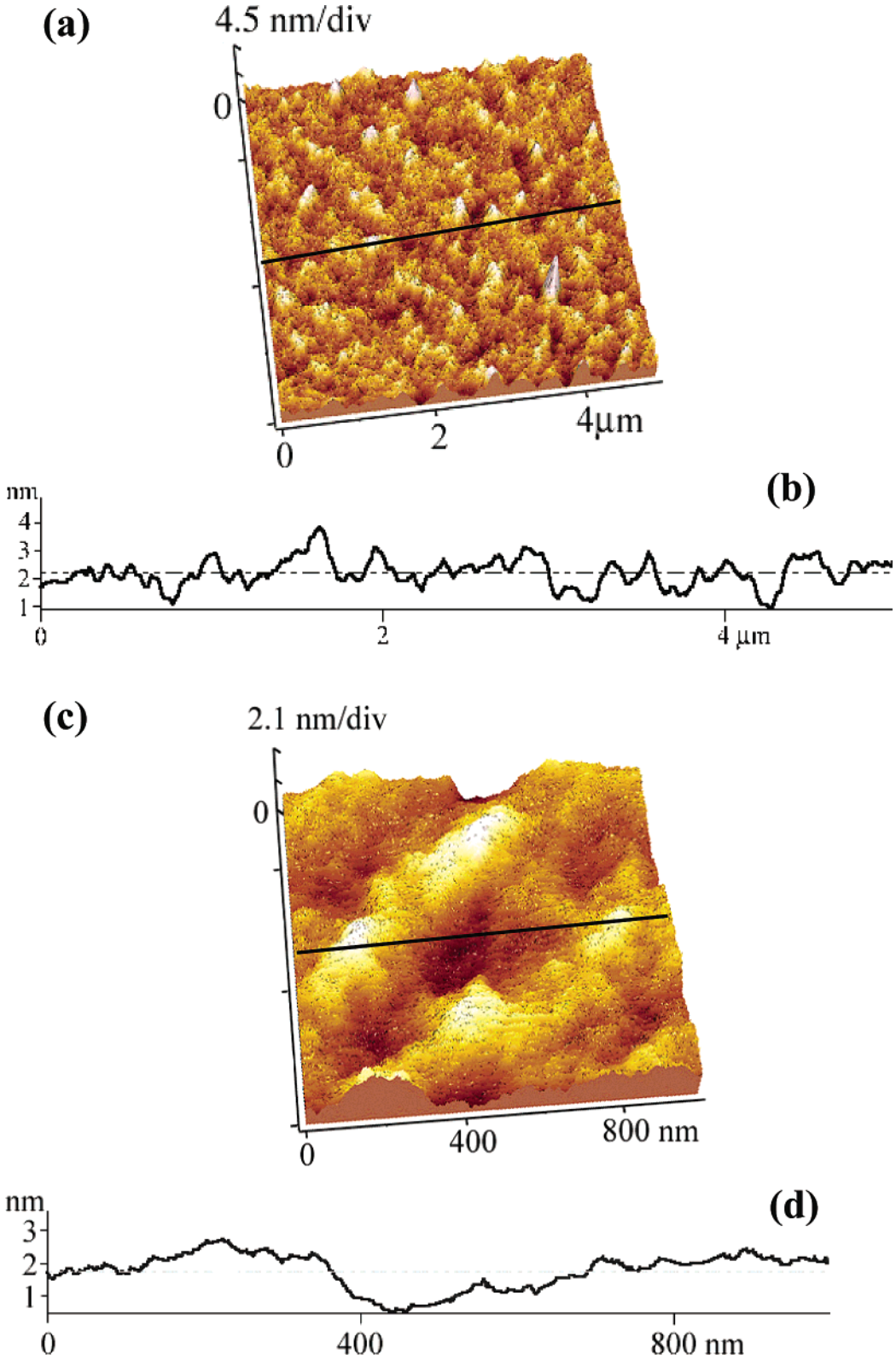

Figure 2. AFM images and surface profiles of an unrubbed C4-PMDA-PDA PI film: (a) image taken with a view angle (scan size 5 × 5 μm^2); (b) surface profile taken along the line in the image (a); (c) magnified image taken with a view angle (scan size 1 × 1 μm^2); (d) surface profile taken along the line in the image (c).

film becomes thinner. Therefore, the measured Δ_{xy-z} value is attributed to the in-plane orientation of polymer chains in PI films. The Δ_{xy-z} value is positive, indicating that the PI polarization is larger along the polymer chain axis than along the direction normal to the polymer chain axis; namely, the PI is a positively birefringent polymer.

To obtain information about the reorientation of polymer chains by the rubbing process, PI films approximately 200 nm in thickness were rubbed and their optical phase retardation was measured. Figure 4 displays a polar diagram of the signal with respect to the angle of rotation of a film rubbed with a rubbing density of 180; here, signal = [(birefringence) × (phase)]

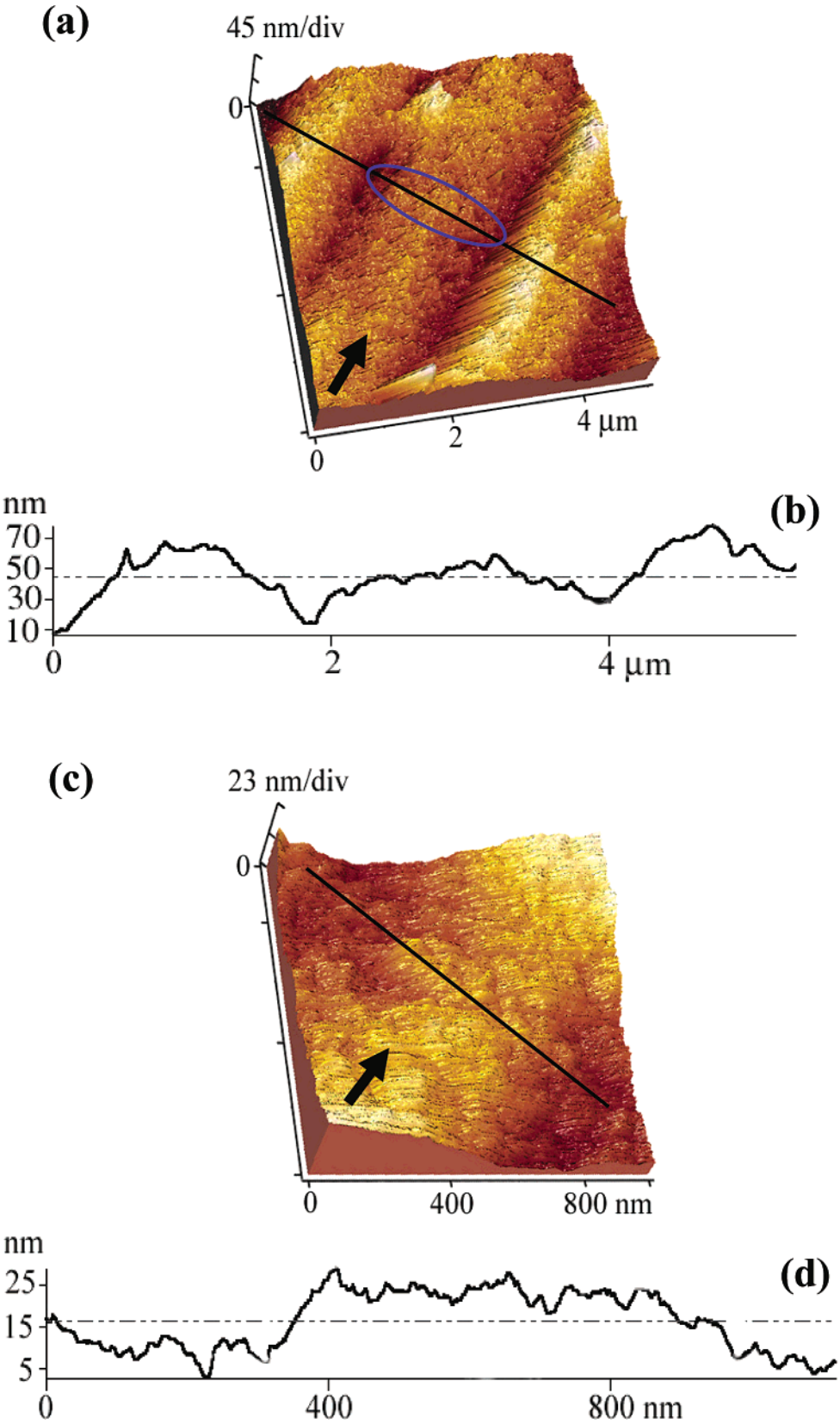

Figure 3. AFM images and surface profiles of a C4-PMDA-PDA PI film rubbed with a rubbing density of 180: (a) image taken with a view angle (scan size 5 × 5 μm^2); (b) surface profile taken along the line in the image (a); (c) magnified image of the elliptical area marked in the image (a); (d) surface profile taken along the line in the image (c). The arrows in the images (a) and (c) denote the rubbing direction, respectively.

in the optical phase retardation measurement. As seen in Figure 4, the rubbed film reveals a maximum signal value along the direction of 180° → 0°, which lies parallel to the rubbing direction, but a minimum signal value along the direction of 90° → 270°, which is perpendicular to the rubbing direction. As described above, the PI chain is positively birefringent. This anisotropic result confirms that the main director of the

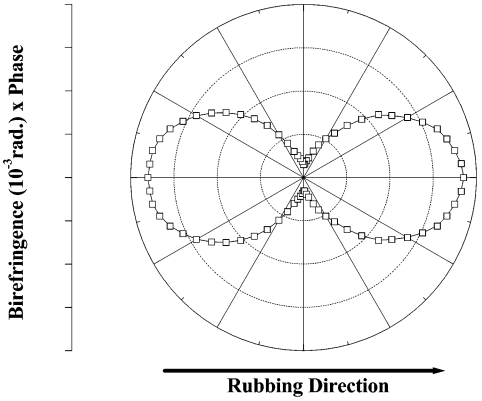

Figure 4. Polar diagram of [(birefringence) × (phase)] (=signal) taken from the optical phase retardation measurement of a rubbed C4-PMDA-PDA PI film as a function of the angle of rotation of the film. The film was rubbed with a rubbing density of 180.

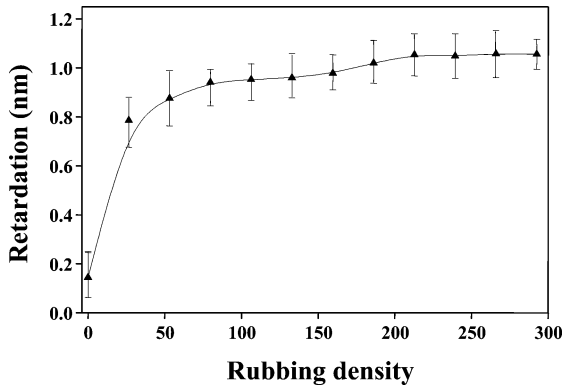

Figure 5. Variation of the optical retardation [=(in-plane birefringence Δ_{xy}) × (film thickness)] of C4-PMDA-PDA PI films rubbed with varying rubbing density.

polymer chains reoriented by rubbing is that parallel to the rubbing direction. In contrast, a polar diagram of signals measured from an unrubbed film of the PI (data not shown) is isotropic with respect to the angle of rotation of the film, confirming that the polymer chains lie randomly in the film plane.

Figure 5 shows the variation of optical retardation with rubbing density, as measured from the PI films. Since retardation = [(in-plane birefringence Δ_{xy}) × (film thickness d)], the variation of retardation in a rubbed film with a thickness d can be attributed to the variation of Δ_{xy} produced by the rubbing process. For the PI film, the retardation (i.e., Δ_{xy}) rapidly increases with rubbing density up to a rubbing density of 60 and then more slowly increases with further increase of the rubbing density, finally leveling off above a rubbing density of 210. These results show that the polymer chains in the surface of the PI film are reoriented along the rubbing direction by the rubbing process and that preferential reorientation can be achieved by rubbing through the rubbing density range 60−210.

In the present study, the rubbing density was varied by changing the cumulative rubbing times for a constant rubbing depth of 1.0 mm. Thus, the retardation variation with rubbing density in Figure 5 shows that the degree of reorientation of polymer chains in the film surface is sensitive to the cumulative rubbing times during early stages and less sensitive at later stages. This result is quite different from that in some earlier reports[26] on flexible types of PI alignment layers, whose

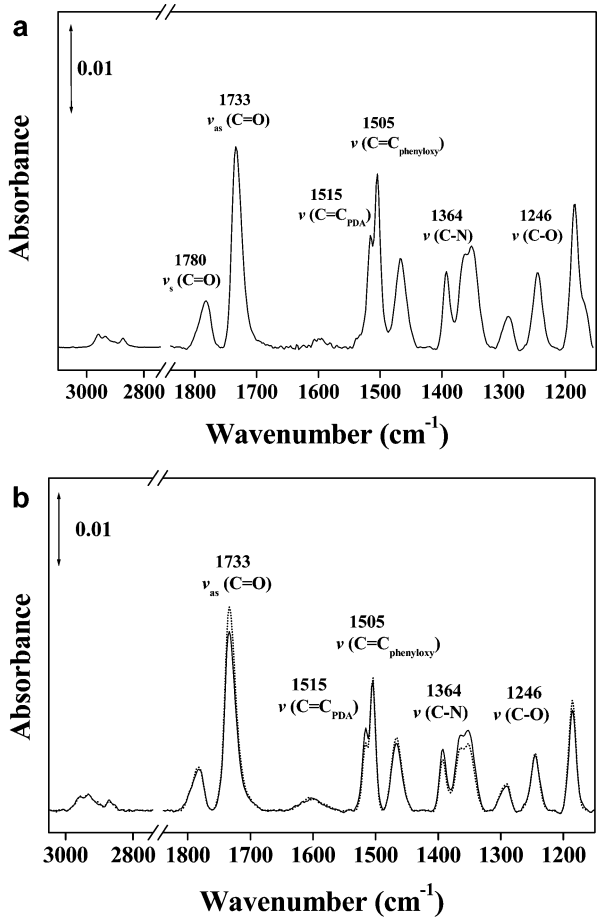

Figure 6. (a) FTIR spectrum of an unrubbed C4-PMDA-PDA PI film measured in transmission mode. (b) FTIR dichroic spectrum from a C4-PMDA-PDA PI film rubbed with a rubbing density of 180. Solid and dashed lines represent the FTIR spectrum with the IR light polarized parallel and perpendicular to the rubbing direction, respectively.

retardation increases only slightly with cumulative rubbing times at a constant rubbing depth.

Molecular Reorientation. Polarized FTIR spectroscopy was used to analyze the molecular orientation of unrubbed and rubbed PI films. In particular, the in-plane orientations of the main chain and side chain subunits on the rubbed PI surface were evaluated. Only modes with in-plane components could be observed in the present study because only normal incidence spectra were measured.

Figure 6a shows an FTIR spectrum obtained from an unrubbed PI film. The vibrational modes obtained from the PI film were assigned with the aid of results previously reported for some other polyimides,[27] and they are summarized in Table 1. Bands at 1780, 1733, 1515, and 1364 cm^{-1} derive from the symmetric and asymmetric C═O stretching vibrations of the imide ring, the C═C stretching vibration of the PDA unit, and the N—C stretching vibration of the imide bond, respectively, all of which are associated with the polymer main chain structure. Additional bands at 1505 and 1246 cm^{-1} are attributed to the C═C stretching vibration of the phenyloxy unit and the asymmetric C—O—C stretching vibration in the side chain, respectively. The stretching vibrations of CH_3 and CH_2 in the side chain appear in the region 3000−2000 cm^{-1}, as listed in Table 1. The asymmetric and symmetric CH_3 stretching vibrations are located at 2958, 2935, and 2872 cm^{-1}. The asym-

Table 1. Characteristic Vibrational Bands of the C4-PMDA-PDA PI

vibrational band (cm^{-1})	assignment
2958	$\nu_{as}(CH_3)$
2935	$\nu_{as}(CH_3)$
2923	$\nu_{as}(CH_2)$
2872	$\nu_{s}(CH_3)$
2852	$\nu_{s}(CH_2)$
1770	$\nu_{s}(CO)$
1733	$\nu_{as}(CO)$
1515	$\nu(C{=}C_{PDA})$
1505	$\nu(C{=}C_{phenyloxy})$
1364	$\nu(N{-}C)$
1246	$\nu(C{-}O)$

metric and symmetric CH_2 stretching vibrational modes are weakly detected at 2923 and 2852 cm^{-1}, respectively; the weakness of these signals is attributed to the relatively low number of these vibrations and to their overlap with the CH_3 vibrations.

In addition, it is noteworthy that the unrubbed PI film reveals no IR dichroism dependence with respect to the rubbing direction. In general, a dichroism dependence (i.e., polarization angle dependence) arises from a preferential molecular orientation in the film plane. The unrubbed PI film is therefore isotropic in the film plane.

Figure 6b presents a representative IR spectrum of a PI film rubbed at a rubbing density of 180, measured with the IR light polarized parallel and perpendicular to the rubbing direction. As seen in the figure, the rubbed film reveals an anisotropy between the IR spectra measured with the IR light polarized parallel and perpendicular to the rubbing direction. Some IR bands (1515 and 1364 cm^{-1}) are more intense when the incident beam is polarized along the rubbing direction. In contrast, other IR bands (1733, 1505, and 1246 cm^{-1}) are enhanced when the polarization is perpendicular to the rubbing direction. Except for the intensity differences in some vibrational peaks which are dependent upon the angle of rotation of the film, the rubbed film exhibits IR spectra which are identical to those of the unrubbed film. The rubbed film exhibits no new vibrational peaks beyond those originating from the PI. If rubbing fibers and polymer chains from the rubbing roll were transferred and deposited onto the rubbed film surface during the rubbing process, as Castellano[8] and Becker et al.[9] suggest, they should be detectable by IR spectroscopy, which has a high sensitivity to the presence of chemical species. Therefore, the possibility of such transfer and deposition of rubbing fibers and their polymer chains onto rubbed PI film surfaces is ruled out by the present study.

In addition to the dichroic IR spectroscopic measurements described above, IR spectroscopic measurements with a linearly polarized IR light source were conducted for the rubbed PI film as a function of the angle of rotation of the film. These measurements were made to determine the extent of reorientation of polymer chains that occurs during the rubbing process. The measured peak intensities of selected IR bands are plotted in Figure 7 with respect to the angle of rotation of the film, as a polar diagram. As seen in Figure 7a and b, the imide N—C band at 1364 cm^{-1} and the C═C band of the PDA unit at 1515 cm^{-1} are more intense when the polarization of the incident beam is parallel to the rubbing direction. Both the imide N—C bond and the PDA unit are parts of the polymer backbone which lie along the main polymer chain axis. Thus, the polar diagrams of both IR bands indicate that the main axis of the polymer chains is reoriented by rubbing to an alignment parallel to the rubbing direction. In contrast, the asymmetric C═O vibration of the imide ring at 1733 cm^{-1} is slightly enhanced when the beam polarization is perpendicular to the rubbing direction (see Figure 7c). The weak effect for this bond could be attributed to the fact that its axis that does not lie exactly perpendicular to the main polymer chain axis, as seen in the chemical structure of Figure 1a. Figure 7c indicates that the asymmetric vibrational mode of the imide C═O bond is more favorably oriented perpendicular to the rubbing direction rather than in other directions. On the other hand, the C—O—C vibration at 1246 cm^{-1} and the aromatic C═C vibration of the phenyloxy unit at 1505 cm^{-1} are enhanced when the beam polarization is perpendicular to the rubbing direction (see Figure 7d and e). These results suggest that the long axis of the phenyloxy unit in the side group is aligned perpendicular to the polymer main chain axis. Unlike the case for the other IR bands described above, polar diagrams for the CH_2 bands could not be constructed because of their weak intensities and their significant overlap with CH_3 vibrational bands. Indeed, no information about the reorientation of *n*-butyl side group ends was obtained from these spectroscopic measurements. However, the reorientation of the *n*-butyl end groups is discussed further in the next section.

LC Alignment. Figure 8a displays a representative polar diagram constructed from the LC cells fabricated with a rubbed film of the PI. As seen in the figure, the main director lies along a direction perpendicular to the rubbing direction, indicating that the LC molecules in contact with the film surface are induced homogeneously to align perpendicular to the rubbing direction. This result suggests that the alignment of LCs on the rubbed PI surface is not directly induced by the microgrooves but by other effects. Taking into account the surface morphology and molecular reorientation results presented above, the data show that the LC molecules are induced to align perpendicular to the microgroove line. The LC alignment is also perpendicular to the polymer main chains, which reoriented preferentially along the rubbing direction and parallel to the direction of the phenyloxy side units, which reoriented in an alignment perpendicular to the rubbing direction. This is the first time that LC molecules in contact with PI films have been found to be aligned perpendicular to the rubbing direction, which is quite different from the LC alignment behavior observed for rubbed films of conventional PI alignment layer materials.

Previously, all rubbed polyimides have been reported to align LCs along the rubbing direction, with the pretilt direction pointing in the rubbing direction.[1−20,26] Rubbed polystyrene (PS), by contrast, was first reported to align LCs perpendicular to the rubbing direction with zero pretilt.[28] This unusual LC alignment has widely been cited as a clue that the microgrooves generated by the rubbing process are not necessarily required to preferentially align LCs at the surface. In the case of PS films, the rubbing process of course generates microgrooves and reorients the vinyl main chains parallel to the rubbing direction, but the phenyl rings are reoriented perpendicular to the rubbing direction. Recently, near-edge X-ray absorption fine structure studies on a rubbed PS film revealed that the reoriented phenyl rings at the surface are positioned in the normal direction with respect to the film plane.[29] This fact suggests that the

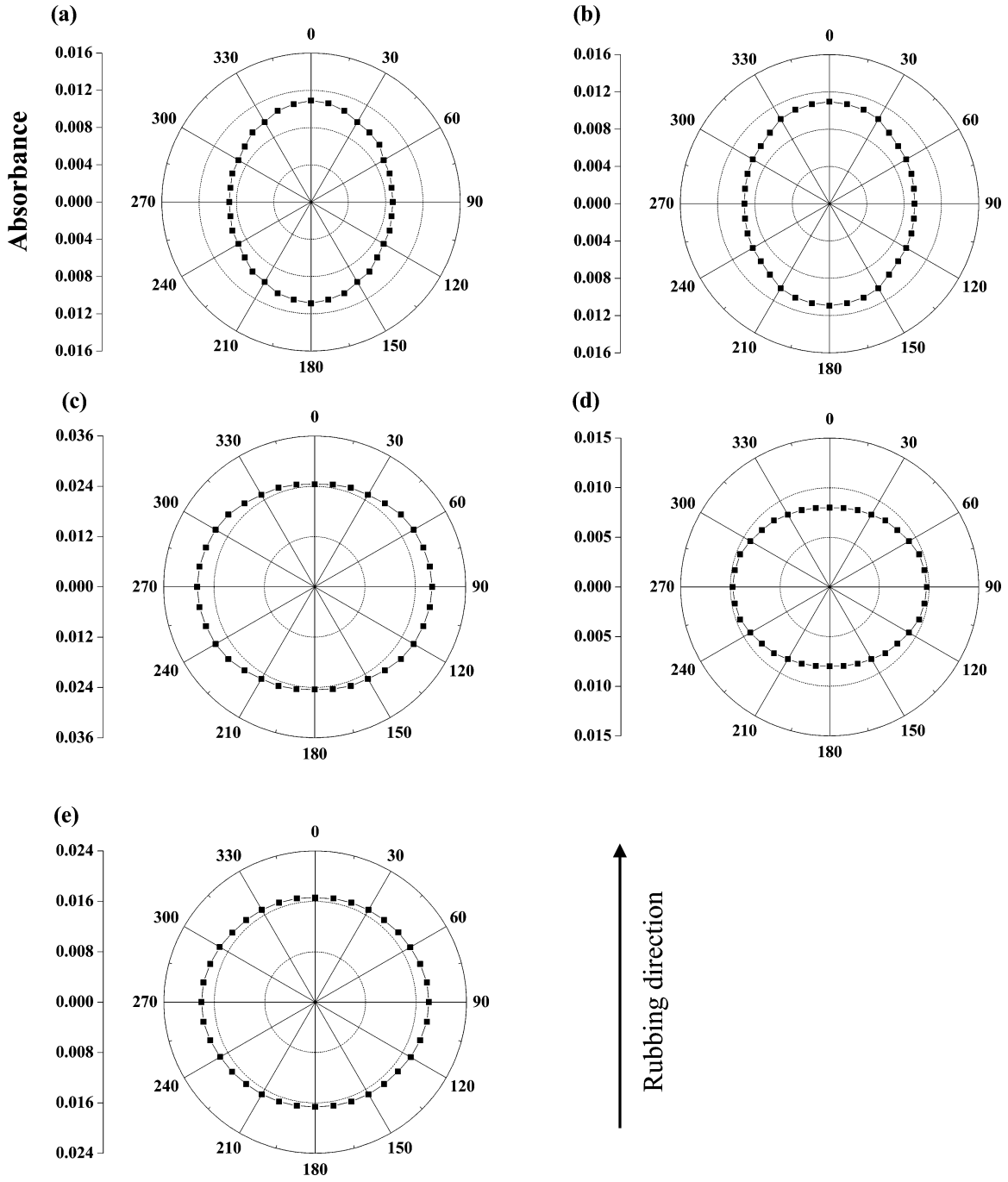

Figure 7. Polar diagrams of some specific vibrational peaks of a C4-PMDA-PDA PI film rubbed with a rubbing density of 180, measured by linearly polarized IR spectroscopy as a function of the angle of rotation of the film: (a) ν(N—C) at 1364 cm^{-1}; (b) ν(C═C_{PDA}) at 1515 cm^{-1}; (c) ν_{as}(C═O) at 1733 cm^{-1}; (d) ν(C—O) at 1246 cm^{-1}; (e) ν(C═$C_{phenyloxy}$) at 1505 cm^{-1}.

observed alignment on the PS surface of LC molecules having an aromatic mesogen unit and an alkyl tail should be attributed to their favorable, strong interaction with the phenyl rings, which overrides the guidance of the unidirectionally developed microgrooves and also their interaction with the vinyl main chains.

Even with consideration of the chemical structure and reorientation of the polymer main chain and its side groups, as well as of the surface morphology, the LC alignment observed in the present study remains a very surprising result. This extreme LC alignment behavior has yet to be explained by any reasonable model.

First, we examine the chemical structure of the PI chain and the surface morphology, and then we consider the possible intermolecular interactions of the polymer chains with LC molecules. The 5CB molecule is ∼1.8 nm in length and ∼0.25 nm in diameter; these dimensions are comparable to those of the chemical repeat unit of the main chain backbone and of the 4-*n*-butoxyphenyloxy side group, which are shown in Figure 1a. In contrast, the microgrooves generated by the rubbing process are a few micrometers in size and their microroughness has a scale of around 100 nm, as discussed above. Even though the microroughness also needs to be considered, the dimensions of these surface structures seem to be too large to effectively interact with and align LC molecules. These facts and the observed LC alignment suggest that the LC molecules are more likely to be aligned by interactions with the polymer main chains and their side groups rather than

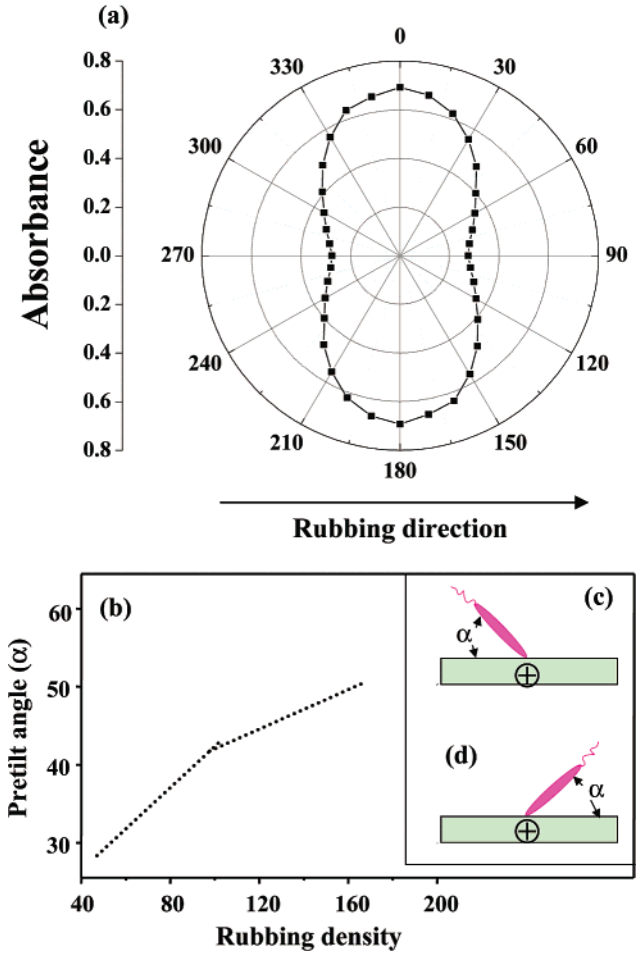

Figure 8. (a) Polar diagram obtained from an LC cell fabricated with a C4-PMDA-PDA PI film rubbed with 180 rubbing density, as a function of the angle of rotation of the LC cell. (b) Variation of the expected pretilt angle of an LC in contact with the rubbed film surface as a function of rubbing density. (c) Possible LC pretilt angle with respect to the left-side direction that is perpendicular to the rubbing direction. (d) Another possible LC pretilt angle with respect to the right-side direction that is perpendicular to the rubbing direction.

by the microgrooves. Only in the case of a weak interaction between the LC molecules and the polymer film might the LC alignment be dominantly governed by the microgrooves and microroughness generated by the rubbing process.

Second, we consider the possible intermolecular interactions between the phenyl ring components of the polymer and the aromatic mesogen unit of the LC molecule. As shown in Figure 1a, in the C4-PMDA-PDA PI, two 4-*n*-butoxyphenyloxy side groups per chemical repeat unit are linked to the 1 and 4 positions of the PMDA unit. Consequently, the entire side group structure consists of the 4-*n*-butoxyphenyloxy group on one side, the phenyl ring of the PMDA unit, and the 4-*n*-butoxyphenyloxy on the other side. The entire side group structure per chemical repeat unit has three phenyl rings, which is one more phenyl ring than the main chain backbone per chemical repeat unit. The phenyl ring of the PMDA unit is of course redundant in both the main chain and the entire side group structure. Thus, the entire side group structure per chemical repeat unit has a better position in intermolecular interactions between the phenyl rings of the polymer and the biphenyl ring of the LC molecule, compared to that of the main chain backbone per chemical repeat unit. Thus, the major intermolecular interactions may be the $\pi-\pi$ interactions between the phenyl rings of the polymer and those of the LC molecule; this has been suggested previously for other PI materials.[19,29,30] If this is the case, then the phenyl rings in the side group structure, which is reoriented by rubbing to an alignment perpendicular to the rubbing direction, contribute to an LC alignment that is perpendicular to the rubbing direction.

Third, the contribution of the imide rings to the intermolecular interaction of the PI with the LC molecules is considered. The main chain backbone of the PI has two imide rings per chemical repeat unit. For each imide ring, the imide N—C bond is a part of the main chain backbone but the two carbonyl C═O bonds are more favorably oriented parallel to the side group rather than to the main chain, as described in the earlier section. The imide carbonyl groups have more polar character than the imide N—C bond, so that the four carbonyl groups per chemical repeat unit may more favorably interact with LC molecules (in particular, with the polar cyano group of 5CB) than do the two imide N—C bonds. This suggests that the reoriented imide carbonyl groups also favor LC alignment perpendicular to the rubbing direction.

Fourth, the entire side group structure also has four ether linkages that the main chain backbone does not have. These ether linkages have a partially polar character and may interact with the LC molecules, resulting in a positive contribution to the LC alignment perpendicular to the rubbing direction.

Finally, we should consider the orientation of the *n*-butyl end groups and their role in LC alignment. We could not obtain any information about the reorientation behavior of the *n*-butyl end groups from our IR spectroscopic study because of the weak absorption intensity of their methylene C—H vibrations and heavy overlapping of these bands with the vibrational peaks of the methyl terminal. Thus, we are restricted to consideration of their chemical and physical characteristics. The *n*-butyl end group consists of only four carbon atoms, which are most stable in the *trans*-conformation. This *n*-butyl end group is sufficiently short that it may have a strong elastic character. When the *n*-butyl end group experiences a shear force created by the fabric fibers during the rubbing process, it may be reoriented along the rubbing direction or some other direction as a result of the shear-induced deformation of the PI chains at the surface. This group may however recover immediately after rubbing to the original conformational position, because of its elastic nature. This would mean that the *n*-butyl end group does not have a distinct reorientation response to the rubbing-induced deformation process but instead takes up an orientation determined by the reorientation of the phenyloxy unit. It is thus suspected that the long axis of the *n*-butyl end group always coincides with the reoriented phenyloxy unit, which takes up orientations perpendicular to the rubbing direction. Because of its aliphatic nature, the *n*-butyl end group may undergo van der Waals type interactions with the aliphatic *n*-pentyl tails of the LC molecules in contact with the rubbed surface, thus also favoring the alignment of LC molecules perpendicular to the rubbing direction.

We conclude that the orientations of the *n*-butyl end groups and of the phenyloxy linkages in the side group play a critical role in the observed LC alignment,

although their role was not determined experimentally. There is indirect support for this statement, as follows. We found that rubbed films of C8-PMDA-PDA PI, which is an analogue of C4-PMDA-PDA PI except for having an *n*-octyl group rather than an *n*-butyl group at the side group end, align LC (5CB) molecules parallel to the rubbing direction.[22,31] In rubbed C8-PMDA-PDA PI films, the *n*-octyl end group was found to be reoriented parallel to the rubbing direction.[31] This result indirectly supports the hypothesis that the long axis of the *n*-butyl end groups in rubbed C4-PMDA-PDA PI films orients perpendicular to the rubbing direction. Indeed, these results lead to the conclusion that alkyl end groups play a critical role in the alignment of LC molecules in contact with the rubbed surface, in addition to the roles played by the other aromatic and polar components of the alignment layer.

Taking the observed LC alignment behavior into account, we used the crystal-rotation technique to try to determine the pretilt angle of the LCs along the direction perpendicular to the rubbing direction, in addition to that along the rubbing direction. However, the LC pretilt angle could not be measured, despite the homogeneous LC alignment. It is well-known that the crystal-rotation technique cannot measure LC pretilt angles over the range 25−55°, due to some limitations in its optical setup. Thus, we suspect that the pretilt angle of LCs in contact with the rubbed C4-PMDA-PDA PI film varies in the range 25−55°, depending upon the rubbing density which is employed in the rubbing treatment of the PI film. The expected variation of the pretilt angle with rubbing density is schematically illustrated in Figure 8b.

On the rubbed C4-PMDA-PDA PI film, the LCs are aligned perpendicular to the rubbing direction, so the pretilt angle should be defined differently than that for other PI films, for which it is in general defined as the angle between the LC molecules and the rubbing direction in a film.[2,3,11−14,17−19] Moreover, the cyano groups of 4-*n*-alkyl-4′-cyanobiphenyl (*n*CB, $n = 1-12$) molecules are known to play a role in keeping the LC molecule close to the surface.[32] On the rubbed C4-PMDA-PDA PI film, the 5CB LC molecule may be pretilted along one of two possible directions, namely the left-side and right-side directions that are perpendicular to the rubbing direction, as indicated in the schematic diagrams shown in Figure 8c and d.

The LC pretilt angle described above is mainly attributed to the side groups that are reoriented perpendicular to the rubbing direction that coincides with the direction of the reoriented polymer chains. The contribution to this LC pretilt angle of the reoriented polymer chains, and of the inclination induced in them by the rubbing process, may be negligible. The LC pretilting result in this study provides support for the claim that the side groups, as well as their *n*-butyl end groups, play a critical role in generating the out-of-plane pretilt angle of the LCs through their intermolecular interactions with the LC molecules.[2,3,11−14,17] For rubbed films of polymers without any side groups, the LC pretilting angle is of course governed by the reoriented polymer main chains and their degree of inclination, but the LC molecules are limited to low pretilt angles. Moreover, when they are reoriented in the same direction by the rubbing process, the reoriented side groups and main chains of a polymer may cooperate in pretilting LCs. Even in this case, the reoriented side groups may contribute more to the LC pretilt angle than does the reoriented polymer main chain.

Taking both the LC alignment results and those for the molecular reorientation of the polymer molecules into account, we suggest a configuration model for the C4-PMDA-PDA PI chains reoriented by the rubbing process and for their alignment of LC molecules. Figure 9 displays a symbolic, schematic configuration model including a representative chain of the reoriented C4-PMDA-PDA PI molecules and two LC molecules aligned by the reoriented polymer chain.

Conclusion

A well-defined brush polyimide composed of aromatic−aliphatic bristles on a fully rodlike backbone, C4-PMDA-PDA PI, was determined to be a positively birefringent polymer. The surface morphology and molecular orientation of the PI in films before and after rubbing were investigated in detail by optical retardation analysis, AFM microscopy, and linearly polarized IR spectroscopy. The LC alignment ability of the rubbed PI films was examined.

For the PI films rubbed for varying cumulative rubbing times with a constant rubbing depth, the optical retardation results suggest that increasing rubbing density via cumulative rubbing times at a constant rubbing depth is a very effective way to produce the reorientation of polymer chains on the film surface. The AFM image analysis of the rubbed film surfaces found that microgroove lines as well as microroughness were formed at the film surface along the rubbing direction. It is evident that each microgroove line is generated by a fiber in contact with the film surface during rubbing, while the microroughness in the microgroove line is created by the subfibrous filaments present at the fiber end. In conclusion, the surface morphology of the rubbed film surface is highly dependent on the detailed structure of the fibers of the velvet fabric employed in the rubbing process, as well as on the rubbing conditions and the shear-induced deformation response of the polymer film. However, the overall surface morphology of the rubbed PI surface was quite different from the morphologies of the rubbed surfaces of ordinary alignment layer materials; in particular, the microroughness within the microgroove line has much smaller surface roughness. These differences might result from the different shear-induced deformation response of this PI film due to its relatively high hardness. In addition, sharp clifflike walls are clearly discernible between the microgroove lines, indicating that some degree of abrasion accompanied the shear-induced PI deformation during the rubbing process.

Despite the positively birefringent characteristic of the PI, its rubbed film induces homogeneous LC alignment perpendicular to the direction of the polymer main chains, which are reoriented preferentially along the rubbing direction that coincides with the microgroove lines and microroughness developed by rubbing. This is the first report of a rubbed PI film aligning LCs perpendicular to the rubbing direction. In contrast, all previously reported rubbed polyimides align LCs along the rubbing direction. This LC alignment behavior is even more surprising when it is taken into consideration that the polymer main chain has some chemical similarity to that of the side group and that it is expected to work cooperatively with the microgrooves and microroughness to produce directionally anisotropic inter-

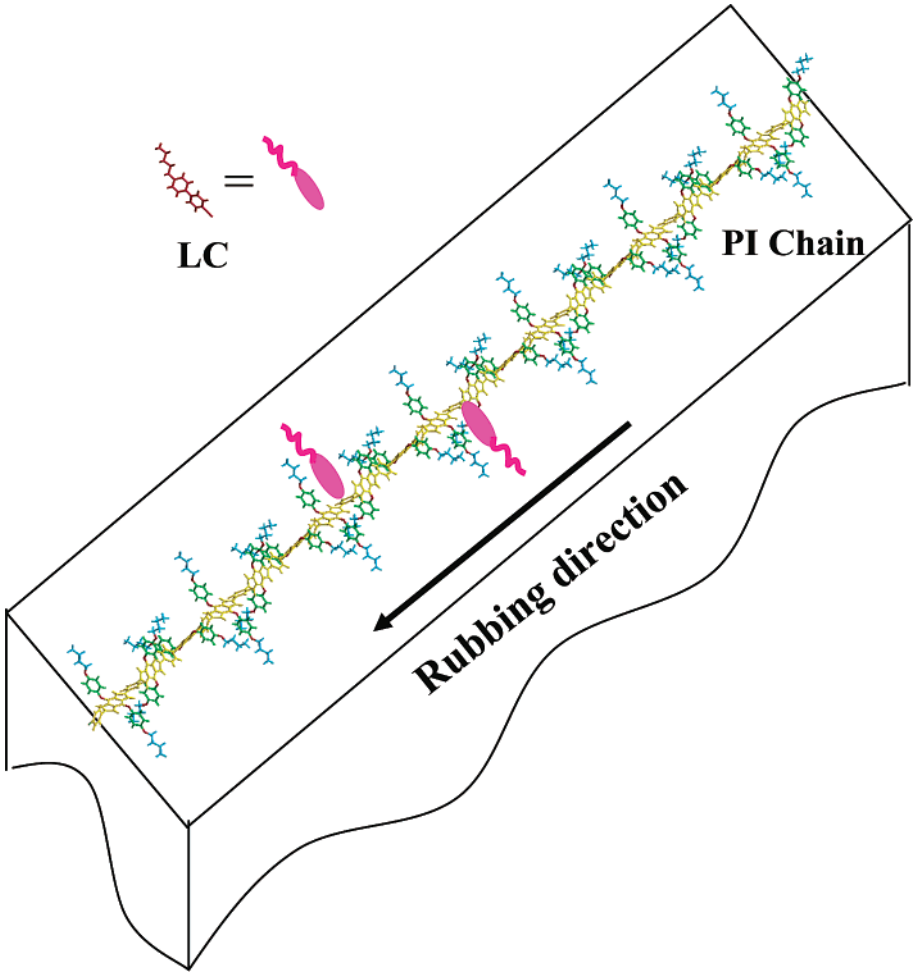

Figure 9. Schematic configuration model of a representative chain of C4-PMDA-PDA PI molecules reoriented at the rubbed film surface, and the LC alignment induced by the polymer molecules.

actions with the LC molecules. This extraordinary alignment of LCs was found to be governed by their anisotropic interactions with the 4-*n*-butoxyphenyloxy bristles and with the imide carbonyl bonds reoriented perpendicular to the rubbing direction, which are stronger than the interactions with the reoriented polymer main chains and the microgrooves and microroughness along the rubbing direction. In addition, it was found that the *n*-butyl end of the bristle plays a critical role in the aligning and pretilting of LCs in contact with the rubbed surface.

This LC alignment result, along with our conclusions as to the surface morphology and the reorientation of polymer chains in the rubbed film, reveals some important features of LC alignment on rubbed polymer surfaces, as follows.

First, LC alignment is predominantly governed by intermolecular anisotropic interactions with all of the directionally reoriented polymer segments rather than by the guidance of and interaction with the microgrooves and microroughness. Only in the case of a polymer having weak intermolecular interactions with LCs are microgrooves and microroughness expected to become the major factor governing LC alignment.

Second, the polymer main chains and the side groups (or side chains) at the rubbed surface cooperatively interact with LCs, when their reorientation directions coincide. Otherwise, they do not cooperate; one competes with the other in alignment of LCs.

Third, the low effectiveness of microgrooves and microroughness in aligning LCs may be attributed to their excessive size, compared to the size (a few nanometers in length and around 0.3 nm in diameter) of LC molecules. If molecular-scaled grooves are formed at the rubbed surface, they might more effectively interact with LCs and make a greater contribution to LC alignment. At present, a velvet fabric made of fibers of around 15 μm diameter is widely used in the mechanical rubbing process, so it is practically impossible to generate microroughness of molecular scale at the film surface. Such molecular-scaled grooves may only be possible when a velvet fabric composed of molecular fibers is employed in the rubbing process.

In conclusion, LC alignment on the rubbed film surface is governed by the dominant factor among the reoriented segments of main chains, the reoriented side groups, and the microgrooves and microroughness, all of whose directionally anisotropic interactions compete to align the LC molecules.

Acknowledgment. This study was supported in part by the Ministry of Industry & Energy and the Ministry of Science & Technology (G7 Project Program), by the KOSEF via the Center for Integrated Molecular Systems and the Center for Advanced Functional Polymers, and by the Korea Research Foundation (BK21 Project).

References and Notes

(1) (a) Collings, P. J., Ed. *Liquid Crystals*; IOP Publishing, Ltd.: Bristol, 1990. (b) Collings, P. J., Patel, J. S., Eds. *Handbook of Liquid Crystal Research*; Oxford University Press: Oxford, 1997.

(2) (a) Lee, K.-W.; Paek, S.-H.; Lien, A.; During, C.; Fukuro, H. *Macromolecules* **1996**, *29*, 8894. (b) van Aerle, N. A. J.; Tol, J. W. *Macromolecules* **1994**, *27*, 6520.

(3) Kim, S. I.; Ree, M.; Shin, T. J.; Jung, J. C. *J. Polym. Sci., Part A: Polym. Chem.* **1999**, *37*, 2909.

(4) (a) Janning, J. L. *Appl. Phys. Lett.* **1972**, *21*, 173. (b) Cognard, J. *Alignment of Liquid Crystals and Their Mixtures*; Gorden & Breach: London, 1982. (c) Mauguin, C. *Bull. Soc. Fr. Miner.* **1911**, *34*, 71.

(5) Geary, J. M.; Goodby, J. W.; Kmetz, A. R.; Patel, J. S. *J. Appl. Phys.* **1987**, *62*, 4100.

(6) (a) Berreman, D. W. *Phys. Rev. Lett.* **1972**, *28*, 1683. (b) Berreman, D. W. *Mol. Cryst. Liq. Cryst.* **1973**, *23*, 215. (c) de Gennes, P. G. In *Physics of Liquid Crystals*; Marshall, W., Wilkinson, D. H., Eds.; Clarendon: Oxford, 1974; Chapter 3. (d) Flanders, D. C.; Shaver, D. C.; Smith, H. I. *Appl. Phys. Lett.* **1978**, *32*, 597. (e) Sugimua, A.; Yamanoto, N.; Kawamura, T. *Jpn. J. Appl. Phys.* **1981**, *20*, 1343. (f) Nakamura, M.; Ura, M. *J. Appl. Phys.* **1981**, *52*, 210. (g) Lee, E. S.; Vetter, P.; Miyashita, T.; Uchida, T.; Kano, M.; Abe, M.; Sugawara, K. *Jpn. J. Appl. Phys.* **1993**, *32*, L1436. (h) Pidduck, A. J.; Bryan-Brown, G. P.; Haslam, S.; Bannister, R.; Kitely, I.; McMaster, T. J.; Boogaard, L. *J. Vac. Sci. Technol. A* **1996**, *14*, 1723. (i) Kim, J.; Kumar, S. *Phys. Rev. E* **1998**, *57*, 5644. (j) Mahajan, M. P.; Rosenblatt, C. *J. Appl. Phys.* **1998**, *83*, 7649. (k) Mahajan, M. P.; Rosenblatt, C. *Appl. Phys. Lett.* **1999**, *75*, 3623.

(7) Uchida, T.; Hirano, M.; Sakai, H. *Liq. Cryst.* **1989**, *231*, 95.

(8) Castellano, J. A. *Mol. Cryst. Liq. Cryst.* **1983**, *94*, 33.

(9) Becker, M. E.; Killan, R. A.; Kosmowski, B. B.; Mlynski, D. A. *Mol. Cryst. Liq. Cryst.* **1986**, *132*, 167.

(10) Nazarenko, V. G.; Lavrentovich, O. D. *Phys. Rev. E* **1994**, *49*, R990.

(11) Dubois, J. C.; Gazard, M.; Zann, A. *J. Appl. Phys.* **1975**, *47*, 1270. (b) Miyano, K. *J. Chem. Phys.* **1979**, *71*, 4108. (c) Miyano, K. *Phys. Rev. Lett.* **1979**, *43*, 51. (d) Okano, K.; Murakami, J. *J. Phys. (Paris)* **1979**, *40*, C3−525. (e) Tarczon, J. C.; Miyano, K. *J. Chem. Phys.* **1980**, *73*, 1994. (f) Okano, K.; Matsuura, N.; Kobayashi, S. A. *Jpn. J. Appl. Phys.* **1982**, *21*, L109. (g) Becker, M. E.; Killan, R. A.; Kosmowski, B. B.; Mlynski, D. A. *Mol. Cryst. Liq. Cryst.* **1986**, *132*, 167. (h) Nakajima, K.; Wakemoto, H.; Sato, S.; Yokotani, F.; Ishihara, S.; Matsuo, Y. *Mol. Cryst. Liq. Cryst.* **1990**, *180B*, 223. (i) Feller, M. B.; Chen, W.; Shen, Y. R. *Phys. Rev. A* **1991**, *43*, 6778. (j) Kikuchi, H.; Logan, J. A.; Yoon, D. Y. *J. Appl. Phys.* **1996**, *79*, 6811. (k) Sawa, K.; Sumiyoshi, K.; Hirai, Y.; Tateishi, K.; Kamejima, T. *Jpn. J. Appl. Phys.* **1994**, *33*, 6273. (l) Hasegawa, R.; Yasushi, M.; Sasaki, H.; Ishibashi, M. *Jpn. J. Appl. Phys.* **1996**, *35*, 3492. (m) Sakamoto, K.; Arafune, R.; Ushioda, S.; Suzuki, Y.; Morokawa, S. *Appl. Surf. Sci.* **1996**, *100−101*, 124. (n) Snively, C. M.; Koenig, J. L. *J. Mol. Struct.* **2000**, *521*, 121.

(12) Johannsmann, D.; Zhou, H.; Sonderkaer, P.; Wierenga, H.; Myrvold, B. O.; Shen, Y. R. *Phys. Rev. E* **1993**, *48*, 1889.

(13) Kim, S. I.; Pyo, S. M.; Ree, M.; Park, M.; Kim, Y. *Mol. Cryst. Liq. Cryst.* **1998**, *316*, 209.

(14) (a) Lee, E. S.; Vetter, P.; Miyahita, T.; Uchida, T. *Jpn. J. Appl. Phys.* **1993**, *32*, L1339. (b) Mori, N.; Morimoto, M.; Nakamura, K. *Macromolecules* **1999**, *32*, 1488. (c) Stohr, J.; Samant, M. G.; Luning, J.; Callegari, A. C.; Chaudhari, P.; Doyle, J. A.; Lacey, J. A.; Lien, S. A.; Purushothaman, S.; Speidll, J. L. *Science* **2001**, *292*, 2299. (d) Toney, M. F.; Russell, T. P.; Logan, J. A.; Kikuchi, H.; Sands, J. M.; Kumar, S. K. *Nature* **1995**, *374*, 709. (e) Samant, M. G.; Stohr, J.; Brown, H. R.; Russell, T. P.; Sands, J. M.; Kumar, S. K. *Macromolecules* **1996**, *29*, 8334. (f) Stohr, J.; Samant, M. G.; Cossy-Favre, A.; Diaz, J.; Momoi, Y.; Odahara, S.; Nagata, T. *Macromolecules* **1998**, *31*, 1942. (g) Cossy-Favre, A.; Diaz, J.; Liu, Y.; Brown, H. R.; Samant, M. G.; Stohr, J.; Hanna, A. J.; Anders, S.; Russell, T. P. *Macromolecules* **1998**, *31*, 4957. (h) Weiss, K.; Woll, C.; Bohm, E.; Fiebranz, B.; Forstmann, G.; Peng, B.; Sheumann, V.; Johannsmann, D. *Macromolecules* **1998**, *31*, 1930. (i) Oh-e, M.; Hong, S.; Shen, Y. R. *J. Phys. Chem. B* **2000**, *104*, 7455. (j) Hietpas, G. D.; Sands, J. M.; Allara, D. L. *J. Phys. Chem. B* **1998**, *102*, 10556. (k) van der Vegt, N. F. A.; Muller-Palthe, F.; Gelebus, A.; Johannsman, D. *J. Chem. Phys.* **2001**, *115*, 9935. (l) Binger, D. R.; Hanna, S. *Liq. Cryst.* **1999**, *26*, 1205. (m) Ge, J. J.; Li, C. Y.; Xue, G.; Mann, I. K.; Zhang, D.; Wang, S.-Y.; Harris, F. W.; Cheng, S. Z. D.; Hong, S.-C.; Zhuang, X.; Shen, Y. R. *J. Am. Chem. Soc.* **2001**, *123*, 5768. (n) Ge, J. J.; Xue, G.; Li, F.; McCreight, K. W.; Wang, S.-Y.; Harris, F. W.; Cheng, S. Z. D.; Zhuang, X.; Hong, S.-C.; Shen, Y. R. *Macromol. Rapid Commun.* **1998**, *19*, 619.

(15) Durand, G. *Physica A* **1990**, *163*, 94.

(16) Barbero, G.; Evangelista, L. R.; Madhusudana, N. V. *Eur. Phys. J.* **1998**, *1*, 327.

(17) Sugiyama, T.; Kuniyash, S.; Seo, D.; Hiroyoshi, F.; Kobayashi, S. *Jpn. J. Appl. Phys.* **1990**, *29*, 2045.

(18) (a) Sakamoto, K.; Arafune, R.; Ito, N.; Ushioda, S.; Suzuki, Y.; Morokawa, S. *Jpn. J. Appl. Phys.* **1994**, *33*, L1323. (b) Sakamoto, K.; Arafune, R.; Ushioda, S. *Appl. Spectrosc.* **1997**, *51*, 541. (c) Arafune, R.; Sakamoto, K.; Ushioda, S. *Appl. Phys. Lett.* **1997**, *71*, 2755. (d) Arafune, R.; Sakamoto, K.; Ushioda, S.; Tanioka, S.; Murata, S. *Phys. Rev. E* **1998**, 58, 5914.

(19) Sakamoto, K.; Arafune, R.; Ito, N.; Ushioda, S.; Suzuki, Y.; Morokawa, S. *J. Appl. Phys.* **1996**, *80*, 431.

(20) (a) Jung, J. C.; Park, S.-B. *J. Polym. Sci.: Polym. Chem. Ed.* **1996**, *34*, 356. (b) Jung, J. C.; Park, S.-B. *Polym. Bull.* **1995**, *35*, 423. (c) Kim, H.; Choi, Y.-J.; Jung, J. C.; Zin, W.-C. *Polym. Bull.* **1997**, *38*, 689. (d) Helmer-Metzmann, F.; Rehahn, M.; Schmitz, L.; Ballauff, M.; Wegner, G. *Makromol. Chem.* **1992**, *193*, 1847. (e) Wenzel, M.; Ballauff, M.; Wegner, G. *Makromol. Chem.* **1997**, *188*, 2865. (f) Helmer-Metzmann, F.; Ballauff, M.; Schulz, R. C.; Wegner, G. *Makromol. Chem.* **1989**, *190*, 985.

(21) (a) Harris, F. W.; Hsu, S. L. C. *High Perform. Polym.* **1989**, *1*, 1. (b) Cheng, S. Z. D.; Lee, S. K.; Barley, J. S.; Hsu, S. L. C.; Harris, F. W. *Macromolecules* **1991**, *24*, 1883. (c) Giesa, R.; Keller, U.; Eiselt, P.; Schmidt, H.-W. *J. Polym. Sci.: Polym. Chem. Ed.* **1993**, *31*, 141. (d) Perry, R. J.; Turner, S. R. *J. Macromol. Sci.: Chem.* **1991**, *A28*, 1213. (e) Schmitz, L.; Rehahn, M. *Macromolecules* **1993**, *26*, 4413. (f) Matsuura, T.; Ishizawa, M.; Hasuda, Y.; Nishi, S. *Macromolecules* **1992**, *25*, 3540. (g) Kim, K. Ph.D. Dissertation, Pohang University of Science & Technology, Korea, 1997.

(22) (a) Lee, K. H.; Jung, J. C. *Polym. Bull.* **1998**, *40*, 407. (b) Lee, S. W.; Kim, S. I.; Park, Y. H.; Ree, M.; Lee, K. H.; Jung, J. C. *Mol. Cryst. Liq. Cryst.* **2000**, *349*, 271. (c) Lee, S. W.; Kim, S. I.; Park, Y. H.; Ree, M.; Lee, K. H.; Jung, J. C. *Mol. Cryst. Liq. Cryst.* **2000**, *349*, 279. (d) Jung, J. C.; Lee, K. H.; Sohn, B. S.; Lee, S. W.; Ree, M. *Macromol. Symp.* **2001**, *164*, 227.

(23) Kim, J.-H.; Kumar, S.; Lee, S.-D. *Phys. Rev.* **1998**, *57*, 5644.

(24) (a) Goh, W. H.; Kim, K.; Ree, M. *Korea Polym. J.* **1998**, *6*, 241. (b) Ree, M.; Kim, K.; Chang, H. *J. Appl. Phys.* **1997**, *81*, 698. (c) Ree, M.; Chu, C. W.; Goldberg, M. J. *J. Appl. Phys.* **1994**, *75*, 1410. (d) Ree, M.; Shin, T. J.; Lee, S. W. *Korea Polym. J.* **2001**, *9*, 1.

(25) Ree, M.; et al. Unpublished optical and scanning electron microscopic results.

(26) (a) Kim, Y. B.; Olin, H.; Park, S. Y.; Choi, J. W.; Komitov, L.; Matuszczyk, M.; Lagerwall, S. T. *Appl. Phys. Lett.* **1995**, *66*, 2218. (b) Kim, Y. B.; Ban, B. S. *Liq. Cryst.* **1999**, *26*, 1579. (c) Zhu, Y.-M.; Wang, L.; Lu, Z.-H.; Wei, Y.; Chen, X. X.; Tang, J. H. *Appl. Phys. Lett.* **1994**, *65*, 49.

(27) (a) Shin, T. J.; Lee, B.; Youn, H. S.; Lee, K.-B.; Ree, M. *Langmuir* **2001**, *17*, 7842. (b) Hasegawa, R.; Yasushi, M.; Sasaki, H.; Ishibashi, M. *Jpn. J. Appl. Phys.* **1996**, *35*, 3492. (c) Hietpas, G. D.; Sands, J. M.; Allara, D. L. *Macromolecules* **1998**, *31*, 3374. (d) Li, W. S.; Shen, Z. X.; Zheng, J. Z.; Tang, S. H. *Appl. Spectrosc.* **1998**, *52*, 985. (e) Rabolt, J. F.; Burns, F. C.; Schlotter, N. E.; Swalen, J. D. *J. Chem. Phys.* **1983**, *78*, 946.

(28) Ishihara, S.; Wakemoto, H.; Nakazima, K.; Matsuo, Y. *Liq. Cryst.* **1989**, *4*, 669. (b) Nakajima, K.; Wakemoto, H.; Sato, S.; Yokotani, F.; Ishihara, S.; Matsuo, Y. *Mol. Cryst. Liq. Cryst.* **1990**, *B180*, 223. (c) Seo, D.-S.; at el. *Jpn. J. Appl. Phys.* **1992**, *31*, 2165.

(29) (a) Stohr, J.; Samant, M. G. *J. Electron Spectrosc. Relat. Phenom.* **1999**, *98*, 189. (b) Stohr, J.; Samant, M. G.; Cossy-Favre, A.; Diaz, J. *Macromolecules* **1998**, *31*, 1942.

(30) Wei, X.; Hong, S.; Zhuang, X.; Goto, T.; Shen, Y. R. *Phys. Rev. E* **2000**, *62*, 5160.

(31) Lee, S. W.; et al. Unpublished results.

(32) Zhuang, X.; Wilk, D.; Marrucci, L.; Shen, Y. R. *Phys. Rev. Lett.* **1995**, *75*, 2144.

MA020639I